Evaluation of a fully self-consistent methodology to correct attenuation and differential attenuation at C-band

L.Baldini, E.Gorgucci
Institute of Atmospheric Sciences and Climate – CNR
Rome, Italy

F. Cuccoli
CNIT O.U., Dept. of Electronics and Telecommunications
University of Florence, Florence, Italy

D. Giuli, M. Gherardelli
Department of Electronics and Telecommunications
University of Florence, Florence, Italy

Abstract— **A methodology to correct reflectivity factor and differential reflectivity at C-band for rain attenuation is presented and evaluated. The methodology is based on a full self-consistency condition describing the interrelation between polarimetric measurements and attenuation or differential attenuation along the rain medium. Evaluation is performed both using C-band profiles generated from S-band radar measurements collected by the NCAR S-Pol radar as well as data collected at C-band by the Polar 55C radar in Italy. Evaluation shows improvement in performance with respect to the available techniques. In particular, it shows the capability to remove any systematic bias that could arise from drop size distribution variability from attenuation and differential attenuation estimates.**

I. INTRODUCTION

Polarimetry applied to weather radars is receiving an increasing attention from meteorological services. In Europe, many ongoing programs aim at upgrading national weather radar networks with polarimetry. In this context, Italy can be considered a pioneer, because since the early 1980s, has promoted the study and development of advanced C-band coherent dual linear polarization radars. In Europe, C-band radars were chosen for meteorological applications because of their lower cost resulting from smaller antenna size compared to lower-frequency radars that have the same spatial resolution. Moreover, C-band can be considered a compromise between S- and X-band in terms of non-Rayleigh effects, maximum sensitivity with minimum attenuation of reflectivity, and influence of the backscattering phase shift. On the other hand, quantitative interpretation of echo powers at C-band frequencies requires correction for attenuation to avoid errors in estimating precipitation. Correction techniques that can be adopted on single parameter radars that measure only the reflectivity factor (Z_h) are notoriously unstable. With polarimetric radars capable of measuring reflectivity factor, differential reflectivity (Z_{dr}), and differential phase shift (Φ_{dp}), different and more reliable correction methods can be used.

A simple correction procedure based on a linear relation between Φ_{dp} and attenuation, and differential attenuation as well was proposed [1]. Presently, one of the most popular correction method is the profiling algorithm (henceforth DPC) that adopts the final value constraint provided by cumulative differential phase [2]. In both techniques, a constant coefficient is used to convert Φ_{dp} to cumulative attenuation. An important property of dual polarization measurements in rain is represented by the self-consistency principle [3][4], which asserts that Z_h, Z_{dr}, and K_{dp} vary in a constrained three-dimensional space for a fixed microphysical model. This principle has been employed in several applications, including the correction of attenuation effects at X- and C-band [5][6].

This paper presents an evaluation of a recent correction method based on the self-consistency principle. Evaluation is performed using C-band profiles generated from S-band radar measurements collected by the NCAR S-Pol radar and C-band data collected by the Polar 55C radar in Tuscany and in Rome (Italy).

II. PARAMETERIZATIONS OF ATTENUATION AND DIFFERENTIAL ATTENUATION

The most common parameterization of specific attenuation (α_h) in dB km^{-1} uses a linear relation with the specific differential phase K_{dp}, in unit of deg km^{-1} [1] as

$$\alpha_h\left(K_{dp}\right)=a_h K_{dp} \quad (\text{dB km}^{-1}) \tag{1a}$$

where the coefficient a_h depends on the factors affecting both α_h and K_{dp}, such as DSD, mean shape of raindrops, and temperature. Integrating (1a) in range we obtain the cumulative attenuation on a rain path used as a constraint in the DPC method.

A similar parameterization was also suggested for specific differential attenuation (α_d)

$$\alpha_d\left(K_{dp}\right)=a_d K_{dp} \ , \quad . (\text{dB km}^{-1}) \tag{1b}$$

but performs worse than (1a). An alternative parameterization for α_d relates it to α_h as

$$\alpha_d=\varepsilon\,\alpha_d\,. \tag{2}$$

The joint use of reflectivity and differential reflectivity was also proposed to parameterize α_h and α_d [7].

More recently, taking into account the synergy of radar polarimetric measurements in rain expressed by the self-consistency principle, the following parameterizations using the triplet (Z_h, Z_{dr}, K_{dp}) were proposed as a part of a procedure to correct attenuation and differential attenuation at X-band [5]

$$\alpha_h\left(Z_h,Z_{dr},K_{dp}\right)=a_h Z_h^{b_h} Z_{dr}^{c_h} K_{dp}^{d_h} \quad (\text{dB km}^{-1}) \tag{3a}$$

$$\alpha_d\left(Z_h,Z_{dr},K_{dp}\right)=a_d Z_h^{b_d} Z_{dr}^{c_d} K_{dp}^{d_d} \quad (\text{dB km}^{-1}). \tag{3b}$$

In the previous expressions, Z_h is in unit of mm^6m^{-1}, and Z_{dr} is dimensionless.

All these parameterizations can be derived and studied through simulation with respect to drop size distribution (DSD) and drop-shape model variation. A large number of gamma DSDs (100000 triplets) is simulated, varying the gamma DSD parameters in a wide range (0.5 $<D_0<$3.5 mm, 3$<\log_{10}N_w<$5, and -1$<\mu<$5), and using the constraints of ($10\log10 Z_h$)<55dBZ and rainfall rate less than 300 mm h^{-1}. Fixing a drop axis ratio model, radar measurements are then simulated at C-band (5.4 GHz), assuming the dielectric constant of water at a temperature of 20° C, and a canting angle of drops mean canting equal to zero degrees and standard deviation of 10° [8].

Fig. 1 compares the parameterizations for α_h and α_d, respectively, for the axis ratio model of Pruppacher and Beard [9] (hereafter PB). The advantage of the self-consistent parameterization (3) is evident and can be quantified in terms of normalized standard error (NSE), which is the root mean square error normalized with respect to the mean true value. The NSE in the parameterization of α_h is reduced from 45.0% to 11.3%

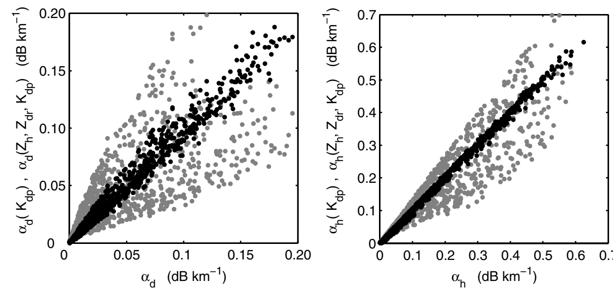

(a) (b)

Figure 1. Scatter plots (a) between α_h and its estimate obtained using parameterizations (1a) and (3a) and (b) between α_d and its estimate obtained using parameterizations (1b) and (3b). Parameterizations based on K_{dp} are represented with gray dots, those based on (Z_h, Z_{dr}, K_{dp}) by black dots.The PB drop-shape model is assumed.

when (3a) is used, while the corresponding NSE in the parameterization of α_d is reduced from 95.5% to 28.2% when (3b) is used instead of (1b).

III. THE FULLY SELF CONSISTENT CORRECTION PROCEDURE

The standard parameterizations (1) have the advantage of using only K_{dp}, which is not affected by attenuation, whereas the self-consistent parameterization (3) use both Z_h and Z_{dr}, which suffer from attenuation effects. To overcome these problems, (3a) and (3b) are rearranged to express K_{dp} in terms of Z_h, Z_{dr}, and α_h (or α_d). Using the preliminary estimates Z_h, Z_{dr}, and α_h (or α_d) obtained by means of DPC and (2), and integrating K_{dp} in range, two preliminary estimates of the reconstructed differential phase are obtained as

$$\Phi_{dp}^h=2\int_{r_0}^{r}\left\{\frac{\alpha_h(s)}{\left[Z_h(s)\right]^{b_h}\left[Z_{dr}(s)\right]^{c_h}}\right\}^{1/d_h} ds \tag{4a}$$

$$\Phi_{dp}^d=2\int_{r_0}^{r}\left\{\frac{\alpha_d(s)}{\left[Z_h(s)\right]^{b_d}\left[Z_{dr}(s)\right]^{c_d}}\right\}^{1/d_d} ds \tag{4b}$$

The differences Δ_h and Δ_d, between the reconstructed and measured differential phase profiles can be minimized as

$$\min(\Delta_h)=\min\left\{\int_{r_0}^{r}\gamma_h\Phi_{dp}^h(s)-\left[\Phi_{dp}(s)-\Phi_{dp}(r_0)\right]ds\right\} \tag{5a}$$

$$\min(\Delta_h)=\min\left\{\int_{r_0}^{r}\gamma_h\Phi_{dp}^h(s)-\left[\Phi_{dp}(s)-\Phi_{dp}(r_0)\right]ds\right\} \tag{5b}$$

where γ_h and γ_d are multiplicative factors, yielding a modified α_h and α_d estimates given by $\tilde{\alpha}_h=\gamma_h^{d_h}\,\alpha_h$ and

$\widetilde{\alpha}_d = \gamma_d^{d_d}\,\alpha_d$. In this way, for a given measured Φ_{dp} profile, the attenuation and differential attenuation profiles estimated from a first guess will be scaled down or up. Different implementations of this approach were proposed [5] [6]. The best performing, described in [6] and referred as FSC (fully self-consistent), is used in this paper.

IV. Evaluation of the Procedure

Attenuation correction procedures cannot be directly tested. Independent measurements of meteorological parameters, compared with corresponding estimates obtained by corrected radar measurements are sometimes used to evaluate indirectly the performance of the attenuation correction procedure. Typically, uncorrected and corrected Z_h and Z_{dr} are used to estimate rainfall rate and the comparison with rain gauge data gives in some way the goodness of the correction procedure [10]. However, using independent measurements collected with different devices can also introduce independent errors that could mask the performances of the different correction procedures. Other techniques use the same corrected radar measurements to establish internal validity for example, using the unaffected K_{dp} measure as a reference of uncorrected and corrected Z_h and Z_{dr} measurements [10] [11] [12]. The correction procedure is evaluated here using both C-band radar measurements and C-band range profiles reconstructed from S-band observations.

A. *Simulation of C-band radar profiles*

S-band profiles used to reconstruct realistic C-band profiles were selected from data collected by the NCAR S-POL radar during two campaigns: i) TEFLUN-B (Central Florida, August 1 - September 30, 1998), an experiment in support of the Ground Validation segment of TRMM; ii) Mesoscale Alpine Programme (MAP) during which S-POL was located at the southern end of the Lago Maggiore (Italy); the Intense Observation Period 02, (September 19-21, 1999) was considered. All 15-km rain paths (the range resolution was 150 m) with an increasing Φ_{dp} along the path greater than 6 degrees were chosen. Following [13], Z_h and Z_{dr} S-band profiles were used to generate realistic profiles of DSD parameters. It was shown [4] that (Z_h, Z_{dr}, K_{dp}) triplets nearly lie on a three-dimensional surface when the drop-shape model is fixed. Therefore, once Z_h and Z_{dr} are specified, the choice of possible K_{dp} values falls in a narrow range. Consequently, for each Z_h and Z_{dr} pair of S-POL profiles, a search of a simulated radar measurement data set built as described in Sect. 2 for S-band provides a possible choice of different DSDs that satisfy the observations. One of those DSDs is randomly chosen and used to build the C-band profiles of Z_h, Z_{dr}, K_{dp}, and the corresponding attenuation and differential attenuation. Signal random fluctuation is also generated in such a way that Z_h, Z_{dr}, and Φ_{dp} measurement errors correspond to 1 dB, 0.3 dB, and 3 degrees, respectively. The differential phase on backscatter, not negligible at C-band, is also considered: It will also have different impact on attenuation correction, because the DPC algorithm uses only one Φ_{dp} measurement whereas the FSC uses the full Φ_{dp} profile. Two datasets are build and referred as FL (Florida) and IT (Italy), depending on the original S-band profiles. Both data sets are generated assuming the PB drop-shape model.

B. *C-band radar measurements*

C-band dual-polarization radar were collected by the coherent dual polarization radar Polar 55C of CNR [14]. The radar operated from 1991 to 2000 in the Montagnana site in Tuscany (Italy) in cooperation with the Departments of Civil and Electronics Engineering of the University of Florence. The system, upgraded with a digital receiver and a new signal processor is operating in the Tor Vergata Research area of CNR in Rome (Italy) since 2001. Two different dataset are considered. The first, referred as the Tuscany data set, was collected during the MAP campaign in fall 1999 in the Montagnana site. The second one (the Rome dataset) was collected in Rome within a campaign conducted throughout the second semester of 2004. Radar measurements were obtained by integrating 64 sample pairs of radar returns at h e v polarizations with a PRF of 1200 Hz. The range resolution was 250 m in the Tuscany data set and 75 m in the Rome dataset.

Data used for evaluation were carefully selected to avoid contamination of the rain radar profile from ground clutter, bright band, and anomalous propagation effects, etc. Range profiles with differential phase increasing along the path greater than 6 degrees were selected. The number of range bins in the path was 100 for the Tuscany data set, and 130 for the Rome data set. The profiles used were 549 and 1560, respectively.

V. Results

The DPC method is implemented with parameterization derived assuming the PB drop-shape model. The coefficients are a_h=0.055 (eq. 1a), ε=0.28, and the exponent of the parameterization of α_h as a function of Z_h used by DPC is 0.823. Parameters of (3) are found assuming a linear shape-size model with the slope varying between 0.04 and 0.08 mm^{-1} to take into account the influence of drop-shape model. Coefficients of (3a) are: a_h=2.546×10^{-5}, b_h=0.776,c_h=-0.340, d_h=0.193. Those of of (3b) are a_d=9.174×10^{-6}, a_d=0.674, c_d=0.804, d_d=0.380.

A. *Simulated profiles*

The DPC and FSC correction procedures are evaluated in terms of normalized bias (NB), which is the difference between the mean estimated and the mean true values normalized to the mean true value, and normalized standard error. Fig. 2(a) shows the NB (thick lines) and NSE (thin lines) of cumulated attenuation estimates (A_h) using the DPC (dashed), and FSC (solid) methods as a function of the rain-path length. Light gray lines correspond to the FL data set and dark grey identify the IT

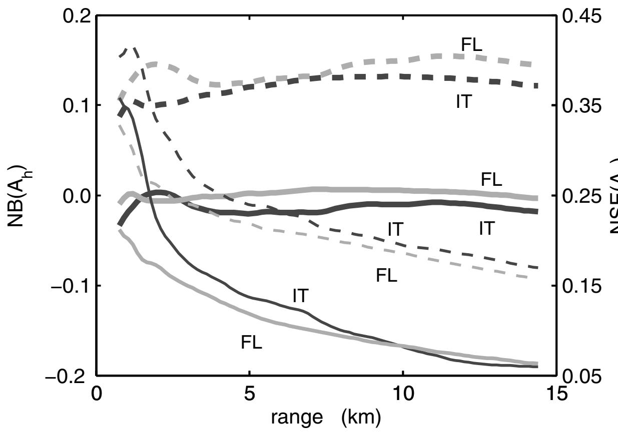

(a)

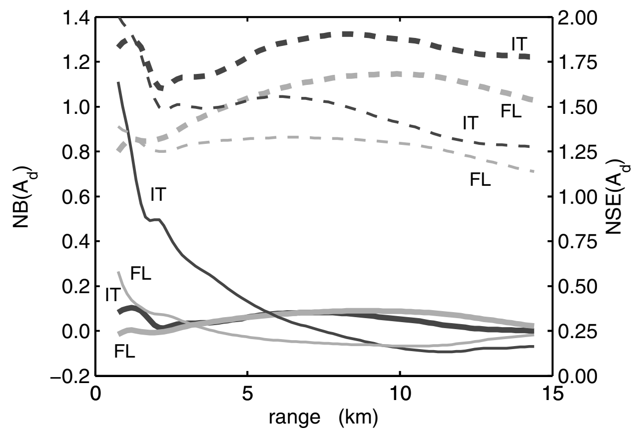

(b)

Figure 2. NB (thick lines) and NSE (thin lines) of (a) cumulative attenuation and (b) cumulative attenuation estimates as a function of the range obtained with FSC (solid) and FSC (dash) for the FL (light gray) and IT (dark gray) data sets.

data set. The figure illustrates the very good performance of A_h estimations with FSC, which is characterized by a NB very close to zero and by a small NSE with averaged values of 23% and 21% for the IT and the FL data sets. It should be noted the attitude of FSC to remove any systematic bias generated by DSD variability along the path. Fig. 2(b) is obtained in the same way and shows the comparison of cumulative differential attenuation (A_d) estimated with the different algorithms compared to the true. Once again, the FSC method shows an ability to remove any bias. In fact, the high bias on the DPC estimates, perhaps due to the considered DSDs that do not account for the used parameterizations, is totally negligible on FSC estimates. Also in this case the performance is characterized by a NB close to 0.

Differently from DPC, FSC is sensitive to biases in Z_h and Z_{dr}. Absolute errors propagate through the attenuation correction procedure and, consequently, as the bias errors increase the performance of SC and FSC decreases. More precisely, when the Z_h and Z_{dr} bias errors assume values of ±1 and ±0.2 dB, respectively, then the NSE of A_h stays within 23% as in the DPC method. The performance for the NSE of A_d is completely different. In fact, NSE for FSC increases to 35%, but remains well below the 147% reached by the DPC method.

B. Polar 55C data

Polarimetric radar data collected with Polar 55C are used to validate the FSC technique in an indirect way, based on statistical comparisons of attenuation and differential attenuation estimates obtained with DPC and FSC with respect to the true values available in the case of reconstructed C-band profiles. Using the reconstructed profiles, the tendency of the relative performances between DPC and FSC is fixed in order to verify if this trend is similar to that where the true values are unknown. Fig 3(a) shows the cumulative frequencies of specific attenuation values estimated with DPC (dashed) and FSC (solid) computed for the FL (light gray) and the IT (dark gray) datasets compared with the cumulative frequencies of the true values (thin black lines with circle and bullet markers, respectively). FSC presents the best performance because it is superimposed onto the true curve for both datasets. Fig 3(b) shows the same curve for the measured datasets. The curve of the Rome dataset shows a slower increase, also due to the shorter pulse width which produces values less smoothed in space. Comparing the relative differences in frequency between FSC and DPC estimated values obtained for simulated and measured datasets, reveals the same trend - DPC increases less slowly than FSC. This common characteristic allows us to think that the true attenuation frequency should be located for the measured dataset as for the simulates dataset. The same speculation can be made for cumulative frequencies of differential attenuation [Fig. 3(c),(d)]. The analysis on cumulative frequencies of differential attenuation reveals a behavior very similar to those of attenuation, allowing allows us to express the same conclusions for the performance of the FSC methodology in estimating differential attenuation.

VI. CONCLUSIONS

A methodology based on the self-consistency principle for the correction of attenuation and differential attenuation suffered by Z_h and Z_{dr} measurements is proposed and evaluated. The quantities Z_h, Z_{dr}, Φ_{dp}, α_h, and α_d are used jointly in a synergetic way to find the best estimate of specific and cumulative attenuation as well as of specific and cumulative differential attenuation, producing highly accurate estimates. The focal result is the inner capability of the method to remove any systematic bias that could arise from DSD variability along the path referred to the used parameterizations.

REFERENCES

[1] V.N. Bringi, V. Chandrasekar, N. Balakrishnan, and D.S. Zrnić, "An examination of propagation effects in rainfall on radar measurements at microwave frequencies," J. Atmos. and Oceanic Technol., vol. 7, pp. 829–840, Dec. 1990.

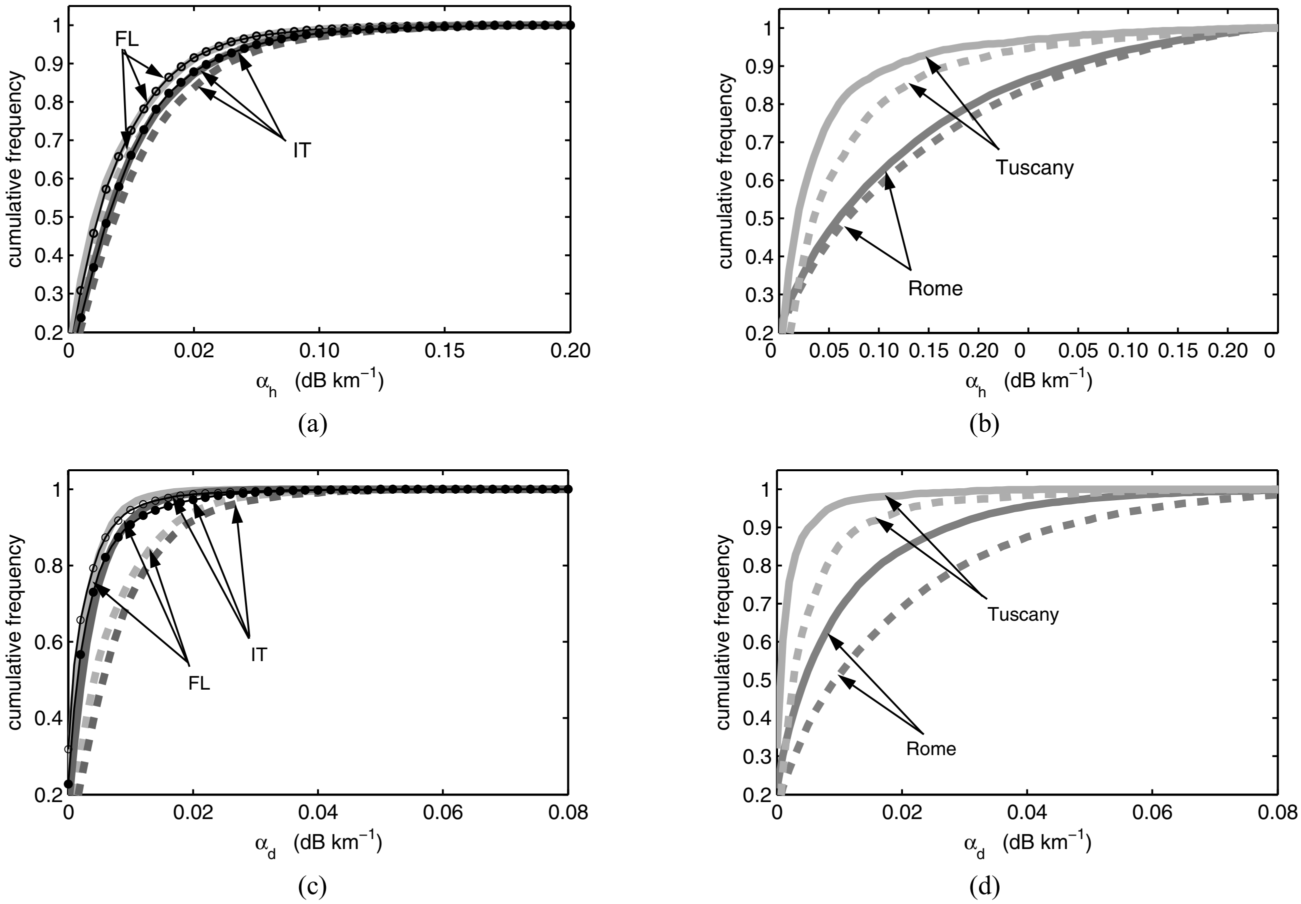

Figure 3. Cumulative frequencies of specific attenuation estimates for the (a) FL (dark grey), IT (light gray), (b) Rome (dark gray), and Tuscany (light gray) data sets obtained using and FSC (dash) and DPC (solid). Cumulative frequencies of true values are indicated by thin black lines with circle and bullet markers for the FL and MAP datasets, respectively. (c) and (d) show the corresponding plots of cumulative frequencies of differential attenuation estimates.

[2] J. Testud, E. Le Bouar, E. Obligis, and M. Ali-Mehenni, "The rain profiling algorithm applied to polarimetric weather radar," J. Atmos. Oceanic Technol., vol 17, pp. 332–356, Mar. 2000.

[3] E. Gorgucci, G. Scarchilli, and V. Chandrasekar, "Calibration of radars using polarimetric techniques," IEEE Trans. Geosci. Remote Sens., vol. 30, pp. 853–858, Sep. 1992.

[4] G. Scarchilli, E. Gorgucci, V. Chandrasekar, and A. Dobaie, "Self-consistency of polarization diversity measurement of rainfall," IEEE Trans. Geosci. Remote Sens., vol. 34, pp. 22–26, Jan. 1996.

[5] E. Gorgucci, V. Chandrasekar, and L. Baldini, "Correction of X-band radar observation for propagation effects based on the self-consistency principle," J. Atmos. Oceanic Technol., vol. 63, pp. 1668–1681, Dec. 2006.

[6] E. Gorgucci, and L. Baldini, "Attenuation and differential attenuation correction of C-band radar observations using a fully self-consistent methodology," IEEE Geoscience and Remote Sensing Letters., *in print*.

[7] E. Gorgucci, G. Scarchilli, V. Chandrasekar, P. F. Meischner and M. Hagen, "Intercomparison of techniques to correct for attenuation of C-band weather radar signals," J. Appl. Meteor., vol. 37, pp. 845–853, Aug. 1998.

[8] V. N. Bringi and V. Chandrasekar "Polarimetric Doppler Weather Radar: Principles and Applications. Cambridge, UK: University Press, 2001, 648 pp.

[9] H. R. Pruppacher and K.V. Beard, "A wind tunnel investigation of the internal circulation and shape of water drops falling at terminal velocity in air," Quart. J. Roy. Meteor. Soc., vol. 96, pp. 247-256, Apr. 1970.

[10] L. D. Carey, S. A. Rutledge, D. A. Ahijevych, and T. D. Keenan, "Correcting propagation effects in C-band polarimetric radar observations of tropical convection using differential propagation phase", J. Appl. Meteor., vol. 39, pp. 1405–1433, Sep. 2000.

[11] T. J. Smyth and A. J. Illingworth, "Correction for attenuation of radar reflectivity using polarization data," Quart. J. Roy. Meteor. Soc., vol. 124, pp. 2393-2415, Oct. 1998.

[12] V. N. Bringi, T. D. Keenan, and V. Chandrasekar, "Correcting C-band radar reflectivity and differential reflectivity data for rain attenuation: A self-consistent method with constraints," IEEE Trans. Geosci. Remote Sens., vol. 39, pp. 1906–1915, Sep. 2001.

[13] Chandrasekar V., Lim S., and E. Gorgucci, "Simulation of X-band rainfall observations from S-band radar data." J. Atmos. Oceanic Technol., vol 23, pp. 1195–1205, Sep.2006,.

[14] E. Gorgucci, L. Baldini, and A. Volpi, 2002: Polar 55C: an upgraded instrument for polarimetric radar research, Proc. of the 2nd European Conf. on Radar Meteorol. ERAD, Delft, The Netherlands, 394-399.